Journal of Applied Informatics and Computing (JAIC)
Vol.9, No.3, June 2025, pp. 583~591
e-ISSN: 2548-6861

IoT-Based Smoking Violation Detection System Equipped with Object Detection Using YOLOv5s Algorithm

Audina Amalia Putri [1]*, Indra Hermawan [2]*
* Information Technology and Computer Engineering, Politeknik Negeri Jakarta
audina.amaliaputri.tik20@mhsw.pnj.ac.id [1], indra.hermawan@tik.pnj.ac.id [2]

Article Info

Article history:

Received 2024-09-09
Revised 2025-04-12
Accepted 2025-04-17

Keyword:

MQ-7,
MQ-135,
Smoking Violation Detection System,
Telegram,
YOLOv5s

ABSTRACT

Smoking is a common habit in Indonesia. The Indonesian government has implemented regulations on smoke-free areas, but violations of the smoke-free policy still often occur. Previous studies have developed smoking violation detection system based on the MQ sensor. However, the smoking violation detection system based only on the MQ sensor is less reliable because the detected gas could come from other sources. Therefore, this study discusses a smoking violation detection system that can automatically verify smoking violation activities using the MQ-7 sensor, MQ-135 sensor, and the YOLOv5s algorithm. The MQ-7 sensor that has been calibrated to detect CO in ppm units achieved an accuracy level of 89.84%. The MQ-135 sensor also has successfully detected ammonia and toluene in cigarette smoke in ppm units. The trained YOLOv5s algorithm achieved an average Precision of 91.9%, Recall 83.7%, F1-Score 87.6%, and mAP50 88.3%. The system is equipped with a speaker that will sound automatically after a verified smoking violation occurs and Telegram notifications in the form of text messages and images.

I. INTRODUCTION

Smoking is a habit that is often found in society, especially in Indonesia. It was recorded in 2023 that Indonesia was ranked 15th as the country with the highest smoking rate in the world with a total figure of 32.6% [1]. Smoking can increase the risk of various diseases such as cancer, heart disease, stroke, chronic bronchitis, emphysema, diabetes, cataracts, pneumonia, tuberculosis, and other dangerous diseases [2]. In fact, as many as 1.3 million people die every year due to being passive smokers [3]. To maintain public comfort and health from cigarette smoke, the Indonesian government has established a law on smoke-free areas. This is as regulated in Article 151 Paragraph (1) Law of the Republic of Indonesia Number 17 Year 2023 regarding Health [4] which reads, "Smoke-free areas consist of: a) Health Service Facilities; b) teaching and learning places; c) places for children to play; d) places of worship; e) public transportation; f) workplaces; and g) public places and other designated places." Campus environment as a place for learning process should be included in the category of a smoke-free area. However, in reality, there are still many smoking violations found in campus areas. Ramachandran *et al.* [5] stated that some of the contributing factors included lacks of policy reminders, lacks of support from students and campus academics, and lacks of strict enforcement of the policy.

To improve discipline towards smoke-free rules, previous studies have created smoking violation detection systems based on MQ gas sensors supported by Internet of Things (IoT) technology. However, the research results of Buchari *et al.* [6] showed a problem when the system indicated that cigarette smoke was detected when actually there was no cigarette smoke when the test was carried out. The researchers in the study concluded that this happened because the gas sensor used not only detected cigarette smoke, but also detected gas from other sources. Therefore, it can be concluded that the smoking violation detection system based only on the MQ sensor is less reliable.

Other studies were conducted by [7], [8], and [9] who created an IoT-based cigarette smoke detection system using an MQ gas sensor with output in the form of an audible warning. However, the warning is given immediately if the MQ sensor detects gas levels exceeding a certain threshold.

In fact, just like the previous problem, the gas detected could come from another source. The system cannot yet confirm in advance whether or not a smoking violation has occurred.

Based on the problems that have been explained, the proposed system in this study will implement object detection technology using the YOLOv5s algorithm as an automatic verification system that a smoking violation has occurred when the MQ sensor detects gas exceeding a certain threshold. In addition, the gases detected are carbon monoxide, ammonia, and toluene which are adjusted to the concentration level of each gas in cigarette smoke with the hope that the system can distinguish cigarette smoke from other smoke. That way, it is hoped that the reliability of the system can increase because the system can automatically verify the occurrence of smoking violations. Therefore, this study aims to improve the reliability of smoking violation detection by combining MQ-7 and MQ-135 gas sensors with the YOLOv5s object detection algorithm, compared to methods that rely solely on MQ-based sensors.

II. METHODOLOGY

A. System Design

Figure 1 shows the block diagram of the system that describes the components used and how each component is connected. The hardware components used in this study are MQ-7 sensor, MQ-135 sensor, ADS1115 ADC module, webcam, Raspberry Pi 4 Model B, ISD1820 module, PAM8403 module, and 8Ω speaker. The MQ-7 sensor functions to detect carbon monoxide, while the MQ-135 sensor functions to detect ammonia and toluene. In order for Raspberry Pi to be able to read analog data from MQ sensors, MQ sensors must be connected to the analog-to-digital converter (ADS1115) module because all pins on the Raspberry Pi are digital pins. Another input device is a webcam that functions to capture image data that the YOLOv5s algorithm will later use to detect cigarette or vape objects. The Raspberry Pi 4 Model B functions as a microcontroller that will process input data into output data. The output device consists of an 8Ω speaker that is connected to an ISD1820 module to record, store, and play warning sounds, and a PAM8403 module as an audio amplifier to amplify the sound produced by the speaker. In addition, other forms of output also exist in the form of Telegram notifications in the form of a text message and an image.

In the developed system, gas sensors (MQ-7 and MQ-135) function as the initial detectors by monitoring the concentration of gases typically found in cigarette smoke, such as carbon monoxide, ammonia, and toluene. If the levels of these three gases exceed the preset threshold, the system will activate the camera and run the YOLOv5s algorithm for visual verification. YOLOv5s will check if there is a cigarette or vape object in the captured image. Only if both conditions are met—gas detection and object recognition—the system will send a notification and activate an audible alarm. Thus, the sensor and object detection technologies work sequentially and synergistically, enhancing the accuracy of the system and reducing the likelihood of false positives.

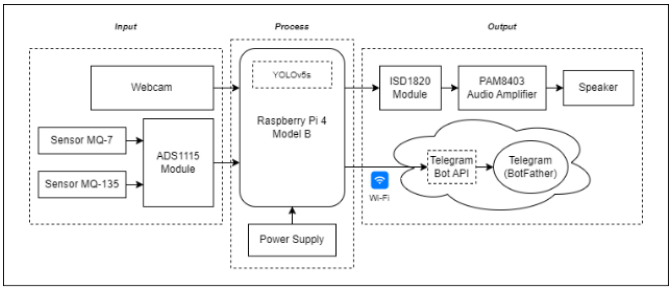

Figure 1. Block diagram of the system

To enhance the system's functionality, the notification system is designed based on the Telegram Bot API, which allows the automatic sending of messages in the form of text and images to specified accounts or groups. These notifications can be customized for various users, such as building managers, security personnel, or campus management, by adding the relevant Telegram account or group IDs to the system configuration. Additionally, the system can be further developed for integration with security devices or building management systems, such as alarms, CCTV cameras, or building control panels, through the use of APIs, webhooks, or protocols like MQTT, enabling a faster and more coordinated response to smoking violations.

Building on the previous explanation, in this system, communication between devices uses the HTTP protocol as the medium for real-time data transmission between the Raspberry Pi and third-party services such as the Telegram API. The Raspberry Pi, acting as the main control unit, processes data from the sensors and detection results from the camera, then sends notifications in the form of images and gas concentration information to Telegram via an internet connection. The system does not use the MQTT protocol as it does not require continuous communication between multiple IoT devices, but instead focuses on event-based notifications. Although a web-based interface has not been implemented in this research, future development could include a web dashboard or mobile application connected to the cloud for remotely monitoring and managing the system, storing violation history, and managing data in a more centralized manner.

Figure 2 shows a flowchart of how the system works. First, the system will perform initialization in the form of hardware activation, network connection, connection between components, import of libraries and modules used, and so on. Then, the system will read the input values from the MQ-7 sensor, MQ-135 sensor, and webcam. If the MQ-7 sensor detects a carbon monoxide concentration of ≥12.22 ppm, the system will then check whether the MQ-135 sensor detects ammonia ≥1.4 ppm. Then, the system will check again whether toluene is ≥0.1 ppm. If all three conditions are met, the system will verify the occurrence of smoking activity through object detection using the YOLOv5s algorithm. If not (one of the gas concentrations does not meet the threshold), it

will re-read the input value. If the camera detects a cigarette or vape object with confidence ≥0.50, the camera will capture a frame (image) and the speaker will sound a warning sound so that smokers can be warned directly on the spot. If not, it will re-read the input value. Next, the system will send a notification to Telegram in the form of a frame (image) that was captured earlier and a text message containing information on the concentration levels of carbon monoxide (CO), ammonia, toluene, and the time of the incident so that the admin can find out if a smoking violation has occurred anywhere and anytime.

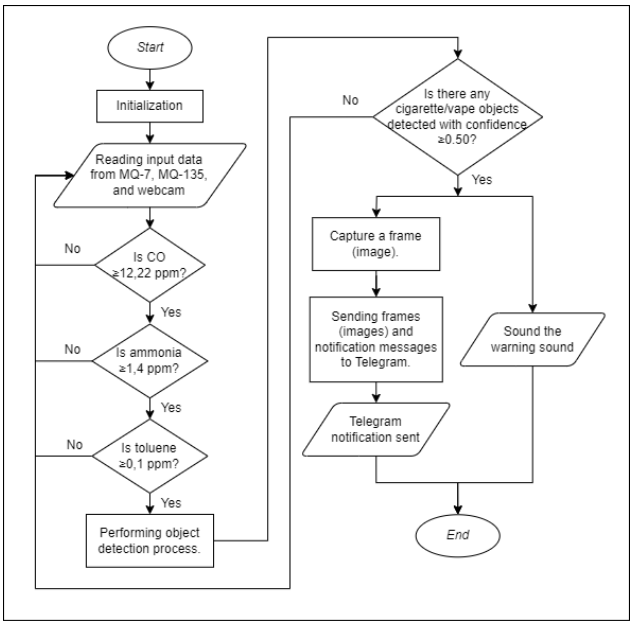

Figure 2. Flowchart of the system

B. MQ-7 Sensor Calibration

To be able to read carbon monoxide content in parts per million (ppm), the MQ-7 sensor must first be calibrated using a simple linear regression formula. Figure 3 shows a graph of the relationship between carbon monoxide gas concentration (ppm) and the voltage output by the MQ-7 sensor (V). According to Muqita *et al.* [10], the voltage output by the MQ-7 sensor is directly proportional to the concentration of carbon monoxide gas. This means that the higher the carbon monoxide gas content, the higher the voltage output by the MQ-7 sensor.

Some of the tools needed to carry out this calibration process are the EZREN DT-9205A digital multimeter to measure the output voltage of the MQ-7 sensor (V) and the AS8700A CO Meter to measure the concentration of CO gas. The MQ-7 sensor and AS8700A CO Meter are placed in a closed glass container, then cigarette smoke is inserted into the container. After that, it will be left until the value read by the CO Meter is stable. Once it is considered stable, the output voltage value of the MQ-7 sensor (V) and the concentration of carbon monoxide gas (ppm) will be recorded. Cigarette smoke will then be added slowly into the container, and the same steps will be repeated.

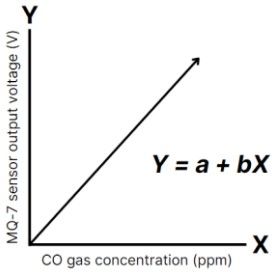

Figure 3. Graph of the relationship between CO gas concentration (ppm) and the output voltage of the MQ-7 sensor (V)

Table I shows the measurement results of the MQ-7 sensor output voltage (V) and carbon monoxide concentration (ppm). The values will be used to calculate the constants a and b as in formulas (1) and (2).

$$a = \frac{(\sum Y)\left(\sum X^2\right) - (\sum X)(\sum XY)}{n\sum X^2 - (\sum X)^2} \quad \ldots (1)$$

$$b = \frac{n(\sum XY) - (\sum X)(\sum Y)}{n\sum X^2 - (\sum X)^2} \quad \ldots (2)$$

After the constant a and constant b values are obtained, the simple linear regression equation formed is $Y = 0{,}959419 + 0{,}0037301X$. This formula will later be implemented in the program code to read the concentration of carbon monoxide gas in ppm units.

TABLE I
MEASUREMENT RESULTS OF MQ-7 SENSOR OUTPUT VOLTAGE (V) AND CO CONCENTRATION (PPM)

No.	Average CO Concentration (ppm)	Average Output Voltage of MQ-7 Sensor (V)
1.	0	0,93479
2.	10,4	0,97187
3.	12,6	1,01083
4.	15,1	1,03934
5.	26,3	1,05366
6.	29,5	1,10361
7.	45,2	1,14366
8.	57,5	1,17894
9.	73,5	1,20016
10.	77,4	1,2535

C. MQ-135 Sensor Calibration

The implementation of the MQ-135 sensor to detect ammonia and toluene refers to the MQSensorsLib library developed by [11] in research entitled "Calibration and Standardization of Air Quality Measurements using MQ Sensors". This library uses a power regression-based formula as in formula (3).

$$ppm = a \times \frac{Rs^b}{Ro} \quad \ldots (3)$$

Rs is the sensor resistance to a particular gas, while Ro is the sensor resistance to clean air.

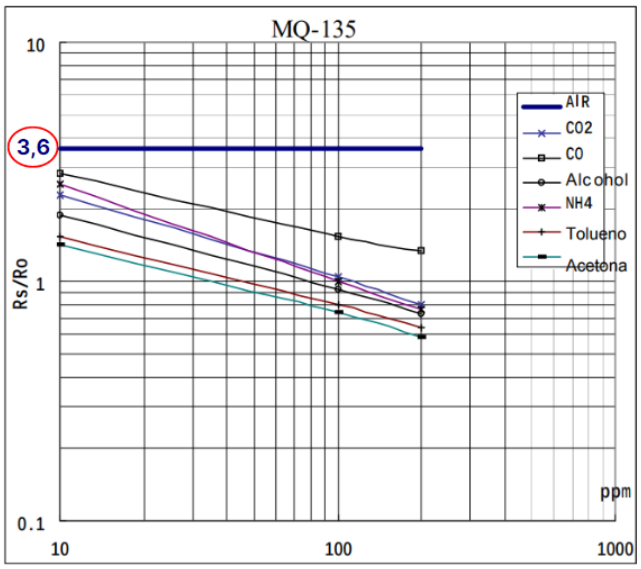

Figure 4. Rs/Ro ratio graph of MQ-135 sensor in clean air based on datasheet

The Rs/Ro ratio of the MQ-135 sensor in clean air is 3,6. This value can be seen in the graph available in the datasheet as shown in Figure 4.

TABLE II
CONSTANT VALUES OF A AND B MQ-135 SENSOR FOR AMMONIA AND TOLUENE BASED ON MQSENSORSLIB LIBRARY

Gas	a	b
Ammonia	102,2	-2,473
Toluene	44,947	-3,445

Based on the MQSensorsLib library, the a and b values of the MQ-135 sensor for ammonia and toluene are shown in Table II, respectively. The MQ-135 sensor must be calibrated in clean air first to determine the Ro value (sensor resistance in clean air). However, to determine the Ro value, the Rs value (sensor resistance in a particular gas) is required, which is searched based on Ohm's law and the voltage division principle as shown in formula (4).

$$Rs = \left(\frac{V_C \times R_L}{V_{RL}}\right) - RL \ldots (4)$$

with
V_C = input voltage (5V)
R_L= load resistance (1 kΩ)
V_{RL}= MQ-135 sensor output voltage

Once the Rs value is known, the Ro value can be found using the formula (5).

$$Ro = \frac{Rs}{3,6} \ldots (5)$$

Finally, the Rs/Ro ratio value is obtained. This value will be used to detect ammonia and toluene gases in parts per million (ppm) using formula (3) which has been explained previously.

D. YOLOv5s Algorithm Implementation

The implementation of the YOLOv5s algorithm consists of dataset creation and model training. The dataset creation stage consists of data acquisition, data preprocessing, data annotation, and data augmentation. The image data collected came from various sources on the internet with details of 3,054 images containing only cigarette objects, 2,685 images containing only vape objects, and 32 images containing both objects (cigarettes and vapes). Thus, the total number of dataset used to train the YOLOv5s model consists of 5,774 images collected from various online sources. These images include cigarette objects, vape devices, and combinations of both, but do not explicitly depict people smoking. The primary focus of the dataset is on the physical appearance of smoking devices, allowing the model to recognize smoking tools in general without relying on human context. The main challenge in training the model lies in handling real-world variations, such as differences in lighting conditions (bright, dim, dark), object distance, viewing angles, and the visual similarity between certain types of vapes and traditional cigarettes. For example, cigalike vapes are difficult to distinguish due to their strong resemblance to regular cigarettes. To address this issue, data augmentation techniques such as adjustments in brightness, exposure, and saturation were applied to improve the model's robustness under varying lighting conditions. In the future, incorporating images of people smoking in real-world contexts could enhance the model's ability to detect smoking violations more contextually and accurately.

(a) Images containing cigarette objects (b) Images containing vape objects

Figure 5. Examples of images in the dataset

Figure 5 shows examples of images for the dataset that were successfully collected from various sources on the internet. The images are divided into training, validation, and test categories with a ratio of 70% training, 20% validation, and 10% test, respectively. The stages of data preprocessing, data annotation, and data augmentation are carried out using Roboflow. The data preprocessing techniques used are auto-orient and resize 640 x 640 (fit black edges in). Auto-orient will maintain the image orientation by ignoring EXIF metadata, thus preventing the image from being displayed upside down, while resize 640 x 640 (fit black edges in) is used to align all images to the same size (640 x 640) by providing black edges so that the image size can be aligned without distorting or changing the aspect ratio. Image

alignment aims to maintain the consistency of the image size used for model training.

TABLE III
EXPERIMENTAL RESULTS OF DIFFERENT AUGMENTATION TECHNIQUES APPLICATION ON THE DATASET

Augmentation Technique	mAP50
Without Augmentation	0,848
Saturation (-25% to +25%) Brightness (-15% to +15%) Exposure (-10% to +10%)	0,881
Saturation (-25% to +25%) Brightness (-15% to +15%) Exposure (-10% to +10%) Noise (0.5% of pixels)	0,874
Saturation (-25% to +25%) Brightness (-15% to +15%) Exposure (-10% to +10%) Noise (0.5% of pixels) Shear (±15° Horizontal, ±15° Vertical)	0,864

To find out the best augmentation technique that can be applied to the dataset, an experiment was conducted as shown in Table III. Based on the results of the experiment, the data augmentation techniques used were saturation (-25% to +25%), brightness (-15% to +15%), and exposure (-10% to +10%) because they achieved the highest mAP50 values.

TABLE IV
YOLOV5S MODEL TRAINING PARAMETERS

imgsz	*batch*	*epochs*	*model*
640	32	500	yolov5s.yaml

YOLOv5s model training was performed on Google Colab. The type of GPU used for model training was NVIDIA GeForce RTX 3090. The model training parameters used are shown in Table IV. Imgsz is a parameter used to determine the size of the image used during model training. The purpose of resizing the image to 640 x 640 is to reduce computational complexity during training. Batch is a parameter that indicates how many images are used during training in one forward pass and backward pass [12]. The selection of the batch size parameter 32 is based on experimental results.

TABLE V
EXPERIMENTAL RESULTS OF DIFFERENT BATCH SIZE PARAMETERS

Batch Size	mAP50	*Training Time*
16	0,881	7,852 hours (7h, 51m, 7s)
32	0,882	6,672 hours (6h, 40m, 19s)

Table V shows the experimental results of applying different batch size parameters to determine the best batch size parameters to use. Based on the experimental results, the batch size parameter 32 produces a model with a mAP50 value 0.113% better than the model trained with the batch size parameter 16. In addition, training the model with a batch size of 32 also has a training time of around 1 hour 10 minutes 48 seconds or 15.03% faster than training using the batch size parameter 16. Therefore, the batch parameters for training the YOLOv5s model in this study use a batch size of 32.

Epochs are parameters used to determine how much the model is trained. One epoch indicates one time the model is trained on all images in the dataset. When the model was trained, the model experienced early stopping at the 433rd epoch because the model did not show any improvement during the last 100 epochs. This means that the model has been trained to its maximum point and if training is continued it will only make the model overfitting. The YOLOv5s model training that has been carried out took 19.874 hours or approximately 19 hours 52 minutes 26 seconds. The training results produce last.pt and best.pt files, each of which is 18.6 MB. The file best.pt will be used in the system.

III. RESULTS AND DISCUSSION

A. MQ-7 Sensor Accuracy Test Results

To determine the error rate and accuracy of MQ-7 sensor in detecting carbon monoxide in parts per million (ppm), testing was carried out to then calculate the Mean Average Percentage Error (MAPE) using formula (6) and accuracy using formula (7). MAPE is a testing parameter used to calculate the level of prediction error against actual data and then multiplied by 100% so that the data can be represented in percentage form [13].

$$MAPE = \frac{1}{n}\sum_{i=1}^{n}\frac{|f_i - y_i|}{y_i} \times 100\% \ldots (6)$$

with
f = MQ-7 sensor reading value
y = AS8700A CO Meter reading value
n = total data

$$Accuracy = 100\% - MAPE \ldots (7)$$

TABLE VI
MQ-7 SENSOR ACCURACY AND ERROR RATE TEST RESULTS

Average CO Reading by MQ-7 Sensor (ppm)	Average CO Reading by AS8700A CO Meter (ppm)	MAPE	Accu-racy
10,543	10,7	1,47%	98,53%
13,813	14,8	6,67%	93,33%
17,492	20,7	15,5%	84,5%
18,71	22,1	15,34%	84,66%
22,039	25	11,84%	88,16%
Average		**10,16%**	**89,84%**

Table VI shows the test results of accuracy and error rate of the MQ-7 sensor to detect CO in ppm units. Based on the test results, the calibrated MQ-7 sensor in this study has an average error rate of 10.16% and an average accuracy rate of 89.84%. This means that the MQ-7 sensor can detect carbon monoxide (CO) levels with a fairly good level of accuracy. However, the calibrated MQ-7 sensor is only effective for detecting carbon monoxide (CO) levels below 15 ppm. This is because when the carbon monoxide (CO) level exceeds 15 ppm, the error rate of the MQ-7 sensor also increases, making

it less effective for use. This can be seen in Figure 6, which shows that after exceeding the carbon monoxide concentration above 15 ppm, the gap in the difference in values read by the MQ-7 sensor and the AS8700A CO Meter increases (indicating an increasing error rate).

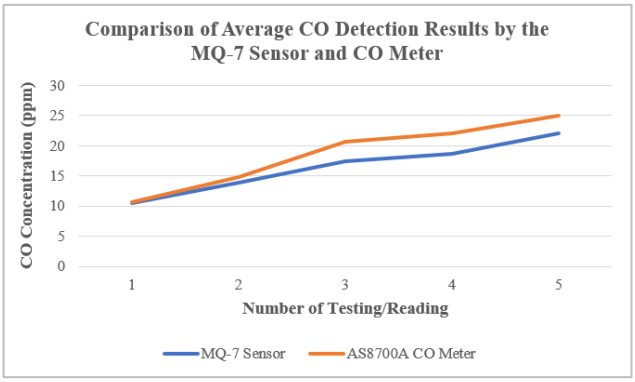

Figure 6. Comparison graph of CO detection results by MQ-7 sensor and CO Meter

B. *MQ-7 and MQ-135 Sensor Functionality Test Results in Detecting CO, Ammonia, and Toluene*

The functional testing of the MQ-7 and MQ-135 sensors aims to determine whether the two sensors can function to detect carbon monoxide, ammonia, and toluene in parts per million (ppm) or not. In addition, by testing various different gases, it can determine the carbon monoxide, ammonia, and toluene content of each type of gas for a concentration of 30 seconds.

TABLE VII
MQ-7 AND MQ-135 FUNCTIONALITY TEST RESULTS IN DETECTING CO, AMMONIA, AND TOLUENE IN PPM UNITS

Types of Smoke	Gas Concentration (ppm)		
	CO	Ammonia	Toluene
Cigarette Smoke	139,93	1,42	0,12
Vape Smoke (Aerosol)	3,86	0,24	0,01
Smoke from Burning Paper	188,54	0,82	0,05
Mosquito Repellent Smoke	179,78	1,03	0,07

Table VII shows the test results of the MQ-7 and MQ-135 sensor functionality in detecting CO, ammonia, and toluene in ppm units. Based on the test results, the MQ-7 sensor and the MQ-135 sensor have successfully functioned to detect carbon monoxide, ammonia, and toluene gases in parts per million (ppm) units in various types or sources of different smoke. Paper-burning smoke has the highest carbon monoxide content, while the highest ammonia and toluene content is achieved by cigarette smoke. On the other hand, vape smoke or commonly referred to as aerosol contains very little carbon monoxide, ammonia, and toluene. This is because the aerosol produced from heating e-liquid tends to contain more propylene glycol and glycerol particles [14].

C. *Precision, Recall, F1-Score, and mAP50 of YOLOv5s Algorithm*

The evaluation metrics of the YOLOv5s algorithm consist of Precision, Recall, F1-Score, and mAP50. Precision is a metric that shows how many model predictions are actually positive samples. Recall is a metric that shows how many samples are true positive and may be predicted by the model correctly [15]. F1-Score is a metric that shows the harmonic mean between Precision and Recall [16]. Mean Average Precision (mAP) is a metric used to measure or show the accuracy performance of an object detection model on all object classes [17].

TABLE VIII
PRECISION, RECALL, F1-SCORE, AND MAP50 RESULTS OF YOLOV5S ALGORITHM

Precision	*Recall*	*F1-Score*	mAP50
0,919	0,837	0,876	0,883

The results of the YOLOv5s algorithm evaluation metrics are shown in Table VIII. Overall, the trained YOLOv5s model has quite good performance as evidenced by the fairly high Precision, Recall, F1-Score, and mAP50 figures. A high Precision value indicates that the model has been quite accurate in detecting positive objects correctly. A fairly high Recall value indicates that the model has been able to detect most of the positive objects. A fairly high F1-Score value indicates that the model has a fairly good balance between Precision and Recall. Finally, a high mAP50 value indicates that the model has high accuracy and precision in predicting the location and position of objects.

D. *YOLOv5s Algorithm Performance Test Results on Distance Variations*

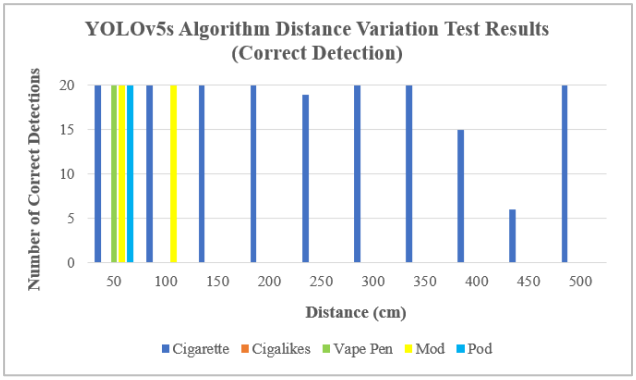

E. F. Figure 7. Graph of YOLOv5s algorithm test results on distance variations (correct detection)

Figure 7 shows the correct detection results of the YOLOv5s algorithm in detecting objects for different distance variations. The cigarette object can still be detected correctly up to the furthest distance, which is 5 meters. Meanwhile, the "mod" vape type can only be detected correctly up to 1 meter. The "vape pen" and "pod" types can only be detected correctly at the closest distance, which is 50 cm. Just like cigarettes, the "cigalikes" type of vape can

actually be detected up to 5 meters. However, because the shape and color are very similar to traditional cigarettes, the model incorrectly classifies it as a “cigarette”, not a “vape”.

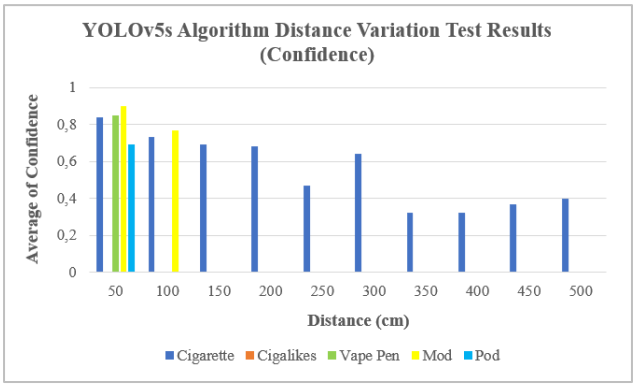

Figure 8. Graph of YOLOv5s algorithm test results on distance variations (confidence)

Figure 8 shows the average confidence results of the YOLOv5s algorithm in detecting objects for different distance variations. It can be seen that the highest confidence for each type of object is achieved at the closest distance, which is 50 cm. This confidence decreases slowly as the distance increases. This is because the closer the object is, the more object details can be captured and processed by the model. The model is also more confident in detecting the object correctly. Conversely, the further the object is, the smaller the resolution produced, and the fewer details can be captured and processed by the model. This can allow important information related to the object to be unreadable, causing the model to be less confident in detecting the object correctly (confidence decreases).

G. YOLOv5s Algorithm Performance Test Results on Light Variations

The performance testing of the YOLOv5s algorithm on light variations was carried out in three different light conditions, namely bright, dim, and dark. Bright lighting conditions are when the lights are on and the window curtains are open, dim lighting conditions are when the lights are off and the window curtains are open, and dark lighting conditions are when the lights are off and the window curtains are closed. It should be noted that the testing was carried out during the day around 12.00-01.00 PM so that even though the lights are turned off, the sunlight source can still enter through the window.

Figure 9 shows the correct detection results of the YOLOv5s algorithm in detecting objects under various lighting conditions. Based on the test results, the trained YOLOv5s algorithm can detect cigarette objects correctly under various lighting conditions, both bright, dim, and dark lighting. However, the model still cannot detect vape objects correctly under dim lighting conditions, let alone dark. The “vape pen” and “mod” vape types can still be detected correctly under dim lighting conditions, but cannot be detected at all under dark lighting conditions. The “pod” vape type can only be detected under bright lighting conditions. Meanwhile, the “cigalikes” vape type cannot be detected correctly at all under various lighting conditions because the model incorrectly recognizes “cigalikes” as traditional cigarettes.

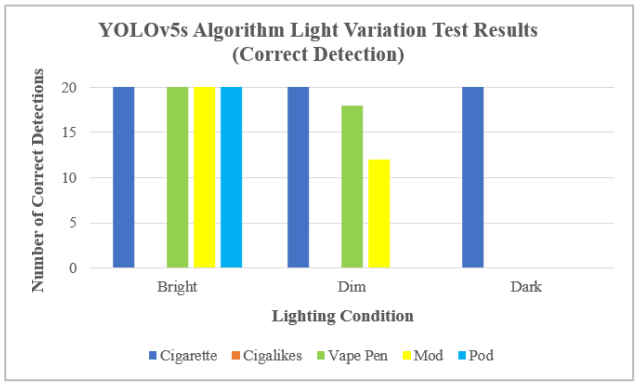

Figure 9. Graph of YOLOv5s algorithm test results on light variations (correct detection)

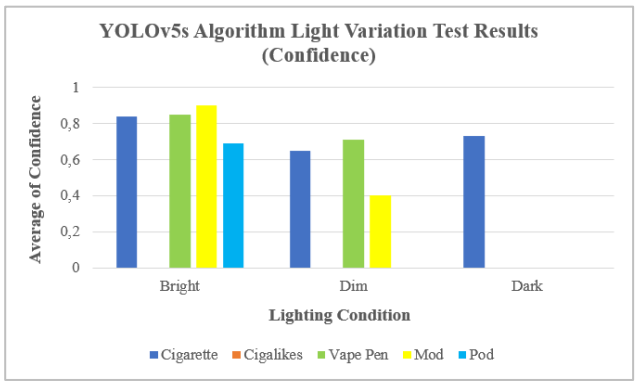

Figure 10. Graph of YOLOv5s algorithm test results on light variations (confidence)

Figure 10 shows the average confidence of the YOLOv5s algorithm in detecting objects under various lighting conditions. In bright lighting conditions, all objects (except cigalikes) can be detected correctly with a relatively high average confidence. However, the average confidence decreases as the light source decreases. This is because in bright lighting conditions, the resulting image has clearer contrast and detail than in dim and dark lighting conditions. The model also finds it easier to recognize important features of the object so that the average confidence can increase. In dim and dark conditions, the light distribution is reduced, causing the resulting image to be blurry, have high noise, or low contrast. This can interfere with the model in detecting objects so that the average confidence produced is lower.

H. Speaker Functionality and Response Time Test Results

Table IX shows the test results of the speaker's functionality and response time. Based on the test results, the speaker has been able to function properly with a 100% success rate. The average speaker response time is in the range of 0.00256 seconds, indicating that the speaker can

sound a warning audio very quickly when smoking activity is detected.

TABLE IX
SPEAKER FUNCTIONALITY AND RESPONSE TIME TEST RESULTS

No.	Status	Response Time (s)
1.	Sounded	0,0025
2.	Sounded	0,0024
3.	Sounded	0,0023
4.	Sounded	0,003
5.	Sounded	0,0025
6.	Sounded	0,0025
7.	Sounded	0,0024
8.	Sounded	0,0024
9.	Sounded	0,0029
10.	Sounded	0,0027
Average		**0,00256**

I. Telegram Notification Functionality and Delivery Time Test Results

Table X and Figure 11 show the Telegram notification test results. Based on the test results, the system has successfully sent Telegram notifications in the form of text messages and images with a success rate of 100% and an average of around 3.531 seconds. This indicates that Telegram notifications were successfully sent with a very low delay. These results were obtained from testing using a Wi-Fi connection that has a download speed of 19.57 Mbps and an upload speed of 6.79 Mbps.

TABLE X
TELEGRAM NOTIFICATION FUNCTIONALITY AND DELIVERY TIME TEST RESULTS

No.	Text Message	Image	Delivery Time (s)
1.	Sent	Sent	3,38
2.	Sent	Sent	3,5
3.	Sent	Sent	3,41
4.	Sent	Sent	3,54
5.	Sent	Sent	3,74
6.	Sent	Sent	3,39
7.	Sent	Sent	3,5
8.	Sent	Sent	3,44
9.	Sent	Sent	3,71
10.	Sent	Sent	3,7
Average			**3,531**

Figure 11. Telegram Notification

IV. CONCLUSION

To assess the practicality and reliability of the proposed system, it is important to critically evaluate whether the achieved results are sufficient for real-world deployment. The test results show that the MQ-7 sensor achieved an average accuracy of 89.84%, which is considered good for detecting carbon monoxide in controlled conditions. However, for more complex real-world environments—such as areas with active ventilation or other sources of pollution—this accuracy may still result in detection errors, especially when CO levels exceed 15 ppm, where the error rate increases significantly.

To address this limitation, the system integrates the YOLOv5s algorithm as a visual verifier, which demonstrates strong performance metrics (Precision 91.9%, Recall 83.7%, F1-Score 87.6%, and mAP50 88.3%). This layered detection approach allows the system to minimize false positives from the gas sensors and false negatives from visual detection. The synergy between these technologies makes the system more reliable and closer to being viable for real-world implementation, although further improvements are still needed, particularly for dynamic and uncontrolled environments.

Although the smoking violation detection system developed in this study demonstrates good performance, there are several limitations that need to be considered, particularly related to environmental conditions. One major challenge is the presence of strong ventilation systems in the monitored area. Active ventilation can disperse or dilute the concentration of gases such as carbon monoxide, ammonia, and toluene, causing the readings from the MQ-7 and MQ135 sensors to become inconsistent or too low to reach the detection threshold. This may lead to the system failing to detect cigarette smoke, especially if the smoke source is shortlived or occurs in open areas with high air circulation.

In addition, the system is vulnerable to smoke from other sources such as kitchen fumes, vehicle exhaust, or burning paper, which may contain gases similar to those found in cigarette smoke. Although the use of YOLOv5s as a visual verifier helps to filter out false positives, camera-based object detection still has its limitations. For instance, in low-light conditions, thick smoke haze, or other visually challenging scenarios, the YOLOv5s algorithm may fail to accurately recognize cigarette or vape objects. Detection can also be hindered if the object (cigarette/vape) is partially hidden or if the user is using a smoking device with an uncommon appearance that was not included in the training dataset. Therefore, the combination of environmental gas factors and object visualization plays a critical role in the system's effectiveness and must be carefully considered when implementing the system in real-world environments.

For future development, it is important to explore the scalability of the system and identify potential challenges when implemented in larger or more crowded environments, such as multi-floor buildings or public transportation hubs. This includes addressing network latency, hardware distribution, and the coordination of multiple detection nodes. Future work should also focus on optimizing response time and notification delivery, particularly in scenarios where real time decisions are critical, such as in educational institutions or healthcare facilities.

In addition, field testing in more realistic environments is essential to evaluate the system's robustness. This includes outdoor or semi-outdoor areas with varying environmental conditions such as wind, temperature fluctuations, humidity, and the presence of other interfering gases. These factors may affect sensor accuracy and object detection performance. Comprehensive field trials would provide deeper insights into system performance, user acceptance, and integration with existing building management or security systems.

ACKNOWLEDGMENTS

Many thanks are expressed to P3M PNJ who have supported and funded this research.

REFERENCES

[1] S. R. Johnson, "These 20 Countries Have the Highest Tobacco Smoking Rates," *U.S. News World & Report*, 2023. https://www.usnews.com/news/best-countries/slideshows/countries-with-the-highest-smoking-rates?onepage (accessed Mar. 08, 2024).

[2] National Cancer Institute, "Harms of Cigarette Smoking and Health Benefits of Quitting," 2017. https://www.cancer.gov/about-cancer/causes-prevention/risk/tobacco/cessation-fact-sheet (accessed Mar. 08, 2024).

[3] World Health Organization, "Tobacco," 2023. https://www.who.int/news-room/fact-sheets/detail/tobacco (accessed Mar. 08, 2024).

[4] Pemerintah Republik Indonesia, "Undang-Undang Republik Indonesia Nomor 17 Tahun 2023 Tentang Kesehatan," *Undang-Undang*, no. 187315, pp. 1–300, 2023.

[5] S. Ramachandran, S. Bentley, E. Casey, and J. P. Bentley, "Prevalence of and Factors Associated with Violations of A Campus Smoke-Free Policy: A Cross-Sectional Survey of Undergraduate Students on A University Campus in the USA," *BMJ Open*, vol. 10, no. 3, pp. 1–10, 2020, doi: 10.1136/bmjopen-2019-030504.

[6] M. A. Buchari *et al.*, "E-WS: A Novel Smart Information System Towards Smokers for the Outdoor Canteen Environment," vol. 172, no. Siconian 2019, pp. 289–293, 2020, doi: 10.2991/aisr.k.200424.043.

[7] S. Kumar, Palnatijayaram, M. Pavan, and P. Lokesh, "No Smoking Zone Monitoring & Alerting System," vol. 12, no. 3, pp. 18–25, 2023.

[8] F. H. Mahdalena, N. Firmawati, and R. Rasyid, "Rancang Bangun Sistem Monitoring Asap Rokok di Toilet Sekolah Menggunakan Sensor MQ-7 dan Transceiver nRF24L01+ dengan Output Suara Berbasis Modul ISD 1820," *Nat. Sci.*, vol. 6, no. 2, pp. 144–150, 2020, [Online]. Available: https://ejournal.uinib.ac.id/jurnal/index.php/naturalscience/article/view/1703.

[9] M. Badrudin, A. Izzuddin, and A. Analisa R, "Rancang Bangun Sistem Peringatan Larangan Merokok Menggunakan Output Rekaman Suara Berbasis Arduino," *J. Sos. Teknol.*, vol. 1, no. 12, pp. 622–631, 2021, doi: 10.59188/jurnalsostech.v1i12.273.

[10] S. G. Muqita, W. Indrasari, H. Suhendar, and M. A. Marpaung, "Karakterisasi Dan Pengujian Sensor Mq-7 Dan Mq-136 Untuk Pengembangan Sistem Monitoring Konsentrasi Gas Karbon Monoksida (Co) Dan Sulfur Dioksida (So2)," vol. XII, pp. 87–92, 2024, doi: 10.21009/03.1201.fa13.

[11] Y. R. Carrillo-Amado, M. A. Califa-Urquiza, and J. A. Ramón-Valencia, "Calibration and Standardization of Air Quality Measurements Using MQ Sensors," *Respuestas*, vol. 25, no. 1, pp. 70–77, 2020, doi: 10.22463/0122820x.2408.

[12] I. Kandel and M. Castelli, "The effect of batch size on the generalizability of the convolutional neural networks on a histopathology dataset," *ICT Express*, vol. 6, no. 4, pp. 312–315, 2020, doi: 10.1016/j.icte.2020.04.010.

[13] A. I. Karisma, F. Kurniawan, and A. Hanani, "Rancang Bangun Sistem Monitoring Environment Area Tempat Tinggal Mahasiswa Berbasis IoT," *Matics*, vol. 11, no. 2, pp. 51–55, 2019, doi: 10.18860/mat.v11i2.8416.

[14] National Academies of Sciences Engineering and Medicine, Health and Medicine Division, Board on Population Health and Public Health Practice, and Committee on the Review of the Health Effects of Electronic Nicotine Delivery Systems, "Toxicology of E-Cigarette Constituents," in *Public Health Consequences of E-Cigarettes*, D. L. Eaton, L. Y. Kwan, and K. Stratton, Eds. Washington (DC): National Academies Press (US), 2018.

[15] A. Tasnim, M. Saiduzzaman, M. A. Rahman, J. Akhter, and A. S. M. M. Rahaman, "Performance Evaluation of Multiple Classifiers for Predicting Fake News," *J. Comput. Commun.*, vol. 10, no. 09, pp. 1–21, 2022, doi: 10.4236/jcc.2022.109001.

[16] S. A. Hicks *et al.*, "On evaluation metrics for medical applications of artificial intelligence," *Sci. Rep.*, vol. 12, no. 1, pp. 1–9, 2022, doi: 10.1038/s41598-022-09954-8.

[17] R. Padilla, S. L. Netto, and E. A. B. Silva, "Proceedings of the 2020 International Conference on Systems, Signals and Image Processing, IWSSIP 2020," *Int. Conf. Syst. Signals, Image Process.*, vol. 2020-July, pp. 237–242, 2020